CrossMark

Electroporation of archaeal lipid membranes using MD simulations

Andraž Polak [a], Mounir Tarek [b,c], Matija Tomšič [d], Janez Valant [e], Nataša Poklar Ulrih [e], Andrej Jamnik [d], Peter Kramar [a], Damijan Miklavčič [a,*]

[a] University of Ljubljana, Faculty of Electrical Engineering, Tržaška cesta 25, SI-1000 Ljubljana, Slovenia
[b] Université de Lorraine, UMR 7565, F-54506 Vandoeuvre-lés-Nancy, France
[c] CNRS, UMR 7565, F-54506 Vandoeuvre-lés-Nancy, France
[d] University of Ljubljana, Faculty of Chemistry and Chemical Technology, Aškerčeva c. 5, SI-1000 Ljubljana, Slovenia
[e] University of Ljubljana, Biotechnical Faculty, Jamnikarjeva 101, SI-1000 Ljubljana, Slovenia

ARTICLE INFO

ABSTRACT

Molecular dynamics (MD) simulations were used to investigate the electroporation of archaeal lipid bilayers when subjected to high transmembrane voltages induced by a charge imbalance, mimicking therefore millisecond electric pulse experiments. The structural characteristics of the bilayer, a 9:91 mol% 2,3-di-O-sesterterpanyl-sn-glicerol-1-phospho-myo-inositol (AI) and 2,3-di-O-sesterterpanyl-sn-glicerol-1-phospho-1′(2′-O-α-ᴅ-glucosyl)-myo-inositol (AGI) were compared to small angle X-ray scattering data. A rather good agreement of the electron density profiles at temperatures of 298 and 343 K was found assessing therefore the validity of the protocols and force fields used in simulations. Compared to dipalmitoyl-phosphatidylcholine (DPPC), the electroporation threshold for the bilayer was found to increase from ~2 V to 4.3 V at 323 K, and to 5.2 V at 298 K. Comparing the electroporation thresholds of the archaeal lipids to those of simple diphytanoyl-phosphatidylcholine (DPhPC) bilayers (2.5 V at 323 K) allowed one to trace back the stability of the membranes to the structure of their lipid head groups. Addition of DPPC in amounts of 50 mol% to the archaeal lipid bilayers decreases their stability and lowers the electroporation thresholds to 3.8 V and 4.1 V at respectively 323 and 298 K. The present study therefore shows how membrane compositions can be selected to cover a wide range of responses to electric stimuli. This provides new routes for the design of liposomes that can be efficiently used as drug delivery carriers, as the selection of their composition allows one to tune in their electroporation threshold for subsequent release of their load.

1. Introduction

Archaea are extremophile organisms that optimally grow in extreme environments. They are grouped into halophiles that grow in high salt concentration, methanogens that grow under anaerobic condition, thermophiles that grow at high temperatures and psychrophilic that grow at low temperatures. The cell membranes of these archaea have a unique composition, a high chemical and a high physical stability [1–3]. Compared to simple phosphatidyl-choline (PC) lipids, archaeal lipids have head-groups formed by sugar moieties, ether linkages instead of ester linkages between the head group and the carbonyl region, and methyl-branched lipid tails [2]. Aeropyrum pernix is an aerobic hyperthermophilic archaea organism that grows in a coastal solfataric vent at Kodakara, Juma Island, Japan. Its optimal growth environment is at temperatures between 363 K and 368 K, pH 7.0 and salinity of ~3.5%. A. pernix cells are spherical with diameters ranging from 0.8 to 1.2 μm [4]. Their membrane is composed of two lipids: 2,3-di-O-sesterterpanyl-sn-glicerol-1-phospho-myo-inositol (AI) and 2,3-di-O-sesterterpanyl-sn-glicerol-1-phospho-1′(2′-O-α-ᴅ-glucosyl)-myo-inositol (AGI) at a molar ratio of 9:91 mol% [5]. The core of both lipids is a 2,3-di-o-sesterterpanyl-sn-glycerol ($C_{25,25}$-archaeol) while the polar heads are inositol for AI and glucose for AGI (Fig. 1).

The lipids forming the membranes of such organisms are as such very good candidates as components of liposomes for drug delivery [2,6]. For such applications however, the drug should be ultimately released when the carrier (liposome) reaches the intracellular milieu [7]. One of the methods that can be used to enhance the drug release from the synthetic liposomes is electroporation [8,9]. Electroporation is a phenomenon that affects the stability of lipid membranes since it disturbs transiently or permanently their integrity when these are subject to high voltages (electric fields) [10]. Such a technique is now routinely used in fields as diverse as biology, biotechnology and medicine [11]. For simple membranes, molecular dynamics (MD) simulations have shown that the main effect of high electric fields is to enhance the membrane permeability due to the formation of

* Corresponding author at: Laboratory of Biocybernetics, University of Ljubljana, Faculty of Electrical Engineering, Trzaska 25, SI-1000 Ljubljana, Slovenia. Tel.: +386 1 4768 456; fax: +386 1 426 46 58.
E-mail addresses: andraz.polak@fe.uni-lj.si (A. Polak), mounir.tarek@univ-lorraine.fr (M. Tarek), matija.tomsic@fkkt.uni-lj.si (M. Tomšič), janez.valant@bf.uni-lj.si (J. Valant), natasa.poklar@bf.uni-lj.si (N.P. Ulrih), andrej.jamnik@fkkt.uni-lj.si (A. Jamnik), peter.kramar@fe.uni-lj.si (P. Kramar), damijan.miklavcic@fe.uni-lj.si (D. Miklavčič).
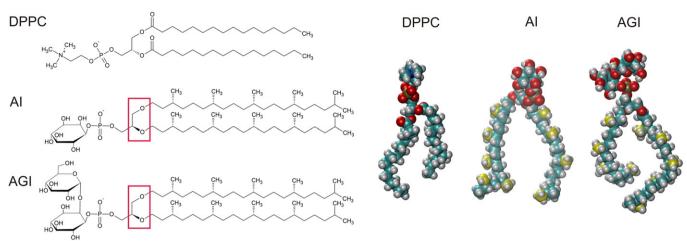
Fig. 1. Representations of archaeal lipids which compose the membrane of Archaea *Aeropyrum pernix* (AI and AGI) and the DPPC lipid.

hydrophilic pores that can be wide enough to transport ions and small molecules [12–17]. When exposed long enough to high fields, lipid bilayers and liposomes can undergo irreversible breakdown [18–20].

Obviously, electroporation of membranes depends on their lipid composition [21]. A molecular level insight about the phenomena has been gathered from MD simulations of lipid bilayers subject to large transmembrane voltages. Most studies concerned the electroporation of phosphatidylcholine (PC) based lipid bilayers [22–26] and the large body of data showed that the electroporation thresholds depend on the type of lipid considered. The presence of increasing cholesterol amounts in lipid membranes was also shown to increase the electroporation threshold [27,28]. Recently, we considered dipalmitoyl-PC (DPPC), and diphytanoyl-PC (DPhPC)-ester and -ether based bilayers [24], comparing therefore lipids with acyl chains and methyl branched chains, and lipids with ether or ester linkages, which changes drastically the membrane dipole potential. We have shown that the electroporation thresholds of these bilayers depend not only on the properties of their component hydrophobic tails but also on the "electrical" properties of the membrane, i.e. its dipole potential.

Archaeal lipids from *A. pernix* present an additional feature: their head group possesses either inositol or glucose moieties. It is unknown how such lipids when forming bilayers would behave under high voltages. It is also interesting to determine how their stability can be modulated by changing the lipid composition, e.g. by adding a third component. This is precisely what we are investigating in the present paper. We first determine the structural characteristics of archaeal lipid bilayers by confronting small angle X-ray scattering data performed on unilamellar vesicles to MD simulations of bilayers of the same composition. We proceed then to study these bilayers electroporation.

2. Material and methods

2.1. Growth of A. pernix K1

The optimum conditions for maximizing *A. pernix* biomass were obtained when $Na_2S_2O_3 \times 5H_2O$ (1 g of per liter) (Alkaloid, Skopje, Macedonia) added Marine Broth 2216 (Difco™, Becton, Dickinson and Co., Sparks, USA) at pH 7.0 (20 mM HEPES buffer) was used as a growing medium in 1 L flask at 365 K (for details see [29]). After growth, the cells were harvested by centrifugation, washed and lyophilized.

2.2. Isolation and purification of lipids, and vesicle preparation

The polar lipid methanol fraction composed of approximately 91% AGI and 9% AI [5] (average molecular mass, 1181.42 g mol^{-1}) was

purified from lyophilized *A. pernix* cells, as described previously [30]. After isolation, the lipids were fractioned using adsorption chromatography [31], and the polar lipid methanol fraction was used for further analysis. Organic solvents were removed under a stream of dry nitrogen, followed by the removal of the last traces under vacuum. For mixed lipid liposomes, the appropriate mass of archaeal $C_{25,25}$ lipids and DPPC were dissolved in chloroform and mixed together in glass round-bottomed flasks. The lipid film was prepared by drying the sample on a rotary evaporator. For preparation of a pure DPPC lipid film, chloroform/methanol (7/3, v/v) was used as solvent. The dried lipid films were then hydrated with warm (~318 K) 20 mmol.l^{-1} HEPES buffer, pH 7.0 or deionized water (milliQ). The mol% of the archaeal $C_{25,25}$ lipids in the mixed archaeal-DPPC liposomes was: 100, 95, 90, 75 and 50. Multilamellar vesicles (MLV) were prepared by vortexing the lipid suspensions vigorously for 10 min. MLV were further transformed into large unilamellar vesicles (LUV). After six freeze (liquid nitrogen) and thaw (warm water) cycles, the liposomes were pressure-extruded 21 times through 400-nm polycarbonate membranes on an Avanti polar mini-extruder (Avanti Polar Lipids, Alabastr, Alabama, USA), at between 323 and 333 K. The total lipid concentration in all SAXS experiments was 10 mg/ml.

2.3. Small-angle X-ray scattering measurements

Small-Angle X-Ray Scattering (SAXS) measurements were performed on the Kratky compact camera (Anton Paar KG, Graz, Austria) [32], which was modified to enclose the focusing multilayer optics for X-rays (Göbel mirror; Osmic). The camera was attached to a conventional X-ray generator Kristalloflex 760 (Bruker AXS GmbH, Karlsruhe, Germany) equipped with a sealed X-ray tube (Cu K$_\alpha$ X-rays with a wavelength $\lambda = 0.154$ nm) and operating at 40 kV and 35 mA. The samples were measured in a standard quartz capillary with an outer diameter of 1 mm and wall thickness of 10 μm. The scattering intensities were detected with the position sensitive detector PSD-50 M (M. Braun GmbH, Garching, Germany) in the small-angle regime of scattering vectors $0.1 < q < 7.5$ nm^{-1}, where $q = 4\pi/\lambda \cdot \sin(\vartheta/2)$, ϑ representing the scattering angle. In order to get reliable measuring statistics, each sample was measured for a period of 20 h. Prior to the data analysis by the inverse Fourier transformation method, the scattering data were corrected for the empty capillary and solvent scattering, and put on the absolute scale using water as a secondary standard [33].

2.4. Evaluation of SAXS data

SAXS data were evaluated using the Indirect Fourier Transformation (IFT) technique [34,35]. Even through the overall dimension of the lipid

bilayer is much above the resolution of the SAXS measurements, we can still extract information about the thickness of the lipid bilayer using such an approach. For this purpose the function $I(q) q^2$, $I(q)$ being the scattering intensity, is cosine transformed into the real space yielding the thickness pair distance distribution function $p_t(r)$ [35–37], which is in the next step transformed into the profile $\Delta\rho_e(z)$ by a convolution square root operation [38–40].

The profile $\Delta\rho_e(z)$ represents the local scattering contrast, i.e. the difference between the local electron density at a distance z from the center of symmetry (central plane in the middle of bilayer) and the average electron density of the sample $\overline{\rho}_e$. Further in the text, the scattering contrast profile $\Delta\rho_e(z)$ will be referred to simply as the electron density profile and denoted as $\rho_e(z)$. In this paper we present only the final SAXS electron density profiles. Details of the evaluation of these SAXS data and other structural SAXS results will be presented elsewhere.

2.5. MD simulations

Morii et al. suggested that two stereo-structures of phospho-myo-inositol (1D and 1L) of AGI may compose the membrane of *A. pernix* [5]. For simplicity we have chosen here to model only the 1D conformation. The AGI and AI molecules were modeled by combining of CHARMM 36 lipids force field (FF) [41] and that of carbohydrates. The FF parameters of ether linkage were adopted from [42].

We considered hydrated bilayers of AI and AGI at a 9:91 molar ratio, and mixed bilayers composed of archaeal lipids + DPPC at 50:50 molar ratio. The MD simulations were carried out using NAMD [43]. The systems were examined at constant pressure ($P = 98$ kPa) and constant temperature (T), or at constant volume (V) and constant T employing Langevin dynamics and the Langevin piston method. The time step for integrating the equations of motion was set to 2.0 fs. Short- and long-range forces were calculated every one and two time steps, respectively. Bonds between hydrogen and heavy atoms were constrained to their equilibrium value. Long-range, electrostatic forces were taken into account using the Particle Mesh Ewald (PME) approach [44,45].

First, a small hydrated bilayer patch (64 lipid molecules spread equally on both leaflets and 10,283 water molecules, 144 potassium (K^+) and 80 chloride (Cl^-) ions) was equilibrated at 323 K for 120 ns. The system was then replicated four times and further equilibrated for tens of ns at 298, 323, 343 and 363 K. These bilayers were composed of 232 AGI and 24 AI molecules. The systems composed of mixtures of archaeal lipids and DPPC in the same ratio were set by replacing half of the archaeal lipids by DPPC molecules (and deleting 128 potassium ions). The latter were equilibrated for tens of ns at 298, 323, 343 K. All the systems were modeled at an ~0.45 mol.l^{-1} KCl solution. In the systems studied at 298 and 343 K, the potassium and chloride ions were removed and replaced by Na$^+$ counter ions to neutralize the overall charge. These systems were used to compare electron density profile determined from simulations to the data derived from SAXS experiments.

The last 15 ns of each simulation had stable average area per lipid; therefore these intervals were assumed as equilibrated runs and were used for the analyses.

The electrostatic potential profiles along the membrane normal was derived from MD simulations using Poisson's equation and expressed as the double integral of the molecular charge density distributions $\rho(z)$:

$$\Phi(z) = -\varepsilon_0^{-1} \iint \rho(z'')dz''dz', \tag{1}$$

z being the position of the charge in the direction along the normal to the bilayer. The dipole potential (U_d) of the bilayers was defined as the electrostatic potential difference between the middle of the bilayer (hydrophobic core) and the bulk (solvent). The transmembrane voltage (U_t) on the other hand was defined as the electrostatic potential

difference between the two bulk regions surrounding the bilayer. The electron density profiles, along the bilayer normal were derived directly from the MD simulations.

The capacitances of the membranes were calculated using the charge imbalance method [46,47]: Selected configurations from the equilibrated NPT (constant pressure and temperature) runs were used to set new systems, where the simulation box size was extended in direction (z) perpendicular to the membrane to create two air water interfaces. For these runs, the temperature was maintained at 298 and 323 K and the volume was maintained constant. Systems with charge imbalances of 0e, 2e, 4e, 6e and 8e were simulated for over 1 ns each. The last 0.5 ns of simulation were used to determine the electrostatic potential distribution, from which the transmembrane voltages (U_t) were calculated. For all simulations, U_t was found in a linear correlation with Q_{im} the charge imbalance normalized to the membrane area. Accordingly the capacitance of the bilayers was estimated as $C_{sp} = Q_{im}/U_t$.

The electroporation of the lipid bilayers was induced by applying high transmembrane voltages using the charge imbalance method. This method mimics the effect of low magnitude microsecond electric pulses [25,47]. The MD simulations of the systems at 298 and 323 K were run at several voltages. The electroporation threshold ($U_{EPthres}$) was reported as interval between the highest U_t at which lipid bilayers are not electroporated in the 100 ns time scale and the lowest U_t at which pores are created in the membrane.

Additional simulations at constant temperature (298 and 323 K) and constant pressure (98 kPa) were performed to estimate the pressure profiles $p(z)$ across the lipid bilayers [48]:

$$p(z) = \frac{1}{\Delta V}\left[\sum_i m_i\mathbf{v}_i\otimes\mathbf{v}_i - \sum_{i<j}\mathbf{F}_{ij}\otimes\mathbf{r}_{ij}f\left(z, z_i, z_j\right)\right], \tag{2}$$

Here $p(z)$ is the local pressure tensor in the slab centered on z, the sum over the kinetic term running over all atoms in the slab and $f(z, z_i, z_j)$ a weighting function. The calculations were all performed on the fly [43].

3. Results and discussion

3.1. Structural characteristics of the bilayers

The time evolutions of the average surface area per lipid molecule (A_m) for archaeal lipid bilayers and their mixtures with DPPC in

Table 1
Properties of the equilibrated archaeal lipids and their mixtures with DPPC bilayers from MD simulations.

Buffer	Bilayer	T/K	t_{sim}/ns	A_m/Å^2	U_d/V	C_{sp}/µF cm^{-2}
0.45 mol l^{-1} KCl	Archaeal lipids	298	53	82.5 ± 0.3	0.23	0.67
		323	31	86.0 ± 0.6	0.23	0.72
		343	25	86.8 ± 0.6	0.20	—
		363	31	90.4 ± 0.7	0.18	—
	Archaeal lipids + DPPC	298	26	69.1 ± 0.7	0.42	0.68
		323	31	72.0 ± 0.9	0.42	0.68
		343	21	73.8 ± 0.7	0.42	—
Na$^+$ counter ions	Archaeal lipids	298	18	83.4 ± 0.4	—	—
		343	33	86.7 ± 0.7	—	—
	Archaeal lipids + DPPC	298	34	68.9 ± 0.4	—	—
		343	23	74.6 ± 0.9	—	—

For comparison the capacitance of DPPC bilayers at 323 K is 0.9 µF cm^{-2} [51] (— not calculated).
T — temperature.
t_{sim} — simulation time.
A_m — area per lipid molecule.
U_d — membrane dipole potential.
C_{sp} — specific capacitance of bilayer.

0.45 mol l^{-1} KCl and in water with Na$^+$ counter ions extracted from the MD simulations performed at different temperatures show that the bilayers were well equilibrated within few tens of ns (data not shown). The obtained molecular and electrical properties of equilibrated membranes are shown in Table 1. The values of A_m are somewhat larger in the archaeal lipid membranes compared with the membranes with mixtures of archaeal lipids and DPPC. They increase with increasing temperature in all studied bilayers. Quite interestingly, the presence of buffer in the systems has practically no effect on A_m.

We have computed the electron density profiles from MD simulations and compared them to those extracted from SAXS data on vesicle samples of the same composition determined at 298 and 343 K to evaluate the quality of the time averaged structure from our simulations. These electron densities (Fig. 2) of each bilayer were found to be in very good agreement. The comparison of profiles of the bilayer in two different buffers estimated from the simulations (data not presented) shows that the buffer has practically no effect on the electron densities of the membrane.

3.2. Dipole potentials

The electrostatic potential profiles across the archaeal lipid bilayers and their mixtures with DPPC were estimated from the charge distribution of their components (cf. methods). The analyses indicate that varying the temperature does not modify the electrostatic potential profiles (data not shown). It is also noticeable that regardless of composition, changes in the temperatures of the systems do not seem to affect much the dipole potential (U_d) of the bilayers (cf. Table 1). However, U_d changes moderately with the lipid composition in particular as DPPC is added. Indeed, archaeal lipid bilayers have a dipole potential

of ~0.2 V and this values almost doubles when DPPC is added at 50 mol%. This dipole potential remains though much smaller than that obtained under similar conditions (force fields and simulation protocols) for pure DPPC bilayers (0.7 V) [24].

3.3. Membrane capacitances

The lipid bilayers were subject to transmembrane voltages (U_t) created using the charge imbalance method. As previously shown, this protocol mimics the effect of low magnitude microsecond electric pulses [25,47]. As depicted in Fig. 3, U_t were found to be proportional to (Q_{im}), the charge imbalance per lipid unit area as found for a variety of other lipid bilayers [24,47,49]. By imposing charge imbalances ranging from 0e to 8e to the modeled systems at 0.45 mol l^{-1} KCl, we have estimated their capacitances [24,47,49]. At 323 K, the latter amount to 0.7 μF cm^{-2} for all lipid bilayers studied here. These values are lower than those of pure DPPC bilayers (0.9 μF cm^{-2}) [24]. This difference is probably mainly rooted in the fact that archaeal lipids, having longer tails, form thicker bilayers. Finally, we found no difference in the capacitances of the bilayers composed of archaeal lipids and their mixtures with DPPC estimated at 298 and 323 K.

3.4. Electroporation thresholds and pores morphologies

We have performed additional simulations at higher charge imbalances and consequently higher transmembrane voltages to trigger electroporation of the bilayers under investigation (cf. Table 2).

Several authors have described MD simulations of zwitterionic (mostly PC based) lipid membranes subject to high transmembrane voltages [12–16]. When the TM voltage is above a threshold value
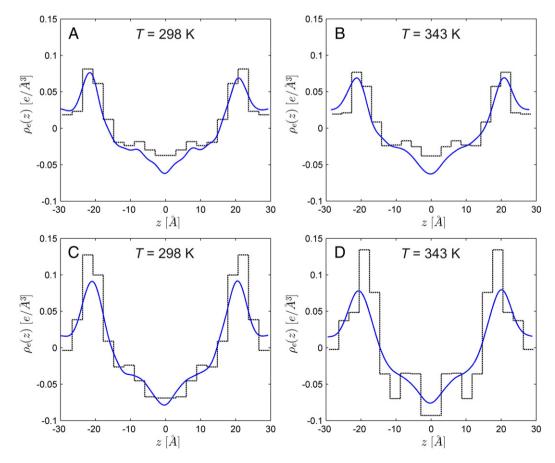

Fig. 2. SAXS derived electron density profiles of liposomes composed of archaeal lipids (A and B) and their mixtures with DPPC (C and D) at 298 and 343 K (dashed black line) and density profiles derived from the MD simulations (blue full line).
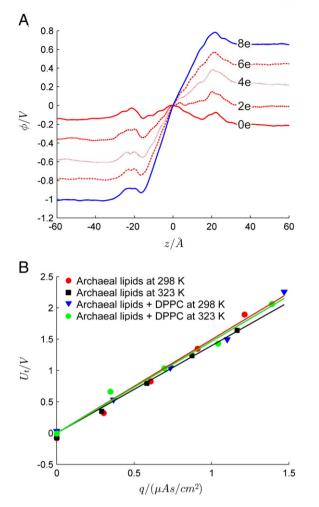
Fig. 3. A) Electrostatic potential profiles (ϕ) across the archaeal lipid bilayers at 323 K (as a function of z distance from the bilayer center) for simulations performed at different net charge imbalances Q (0e to 8e) between the upper and lower electrolytes. B) Transmembrane potentials (U_t) across the archaeal lipids and their mixtures with DPPC bilayers as a function of q, the charge imbalance normalized to the area of bilayers. The slopes represent linear fits to the data that permits estimates of the bilayers capacitances.

Table 2
Electrical and pore characteristics of the archaeal lipids and their mixtures with DPPC in bilayers under various transmembrane voltages created by a net charge imbalance.

Bilayer	T/K	Q_{im}/e	U_t/V	t_{sim}/ns	t_{water}/ns	t_{ion}/ns
Archaeal lipids	298	22	5.0	60	–	–
		24	5.4	59	50.0	58.1
		26	5.9	25	22.1	23.0
		28	6.3	10	7.8	8.4
		30	6.8	3	–	–
	323	20	4.1	61	–	–
		22	4.5	38	26.0	27.4
		24	4.9	10	5.0	6.3
		26	5.3	10	1.2	1.4
Archaeal lipids + DPPC	298	14	3.9	61	–	–
		16	4.3	57	50.5	55.0
		18	4.8	10	5.6	8.7
		20	5.4	10	4.6	5.8
		22	5.9	10	6.1	6.7
		24	6.5	10	1.4	1.6
	323	14	3.6	66	–	–
		16	4.1	23	20.8	22.1
		18	4.6	10	2.8	3.7
		20	5.1	7	2.1	3.3
		22	5.6	10	1.5	1.6

T — temperature.
Q_{im} — charge imbalance.
U_t — transmembrane voltage.
t_{sim} — simulation time.
t_{water} — time when first water wire is formed.
t_{ion} — time when first ions goes through the pore.

characteristic of the lipid composition, the membrane loses its integrity. This enables to increase substantially the ionic and molecular transport through the otherwise impermeable membranes [17]. Electroporation starts with the formation of water fingers that protrude inside the hydrophobic core of the membrane. Within nanoseconds, water wires bridging the two sides of the lipid bilayer appear. If the simulations are further extended, few lipid head-groups migrate along one water wire and form a hydrophilic connected pathway; if the voltage is maintained the ions present in solution start to flow through this pathway from one side of the membrane to the other. If the TM voltage is lowered, or is reduced due to ionic flow across the membrane, the pores collapse to reach a non-solvated and non-conductive state [13,24,25]. It was shown that the full recovery of the membrane integrity (migration of the lipid head groups back to the lipid water interface) requires few tens of nanoseconds.

In the present case (cf Fig. 4), for archaeal lipid bilayers, as reported for zwitterionic membranes, the process of electroporation starts with the protrusion of water fingers from either one or both sides of the membrane. Water defects appear within few nanoseconds then merge to form a complete transmembrane wire. Such a defect, hereafter called a "hydrophobic pore" to indicate that the water columns are in contact with the hydrophobic lipid tails, then expands in width. Surprisingly, in all the trajectories, the pores remained "hydrophobic" i.e. no lipid head groups moved toward the interior of the lipid hydrophobic core along these water wires. Regardless of this nature of the pore, ions were then driven along the electrical gradient (cf Fig. 4). Hence, in contrast to previously reported behavior of PC based lipids, the archaeal lipids forming the bilayer did not migrate toward the interior of the hydrophobic core to stabilize the water conducting pores. A similar behavior was also noted for the systems containing a fraction of DPPC. The series of simulations performed along with the characteristic times: t_{water} (time when the first water wire was created in the lipid bilayer) and t_{ion} time at which the first ions went through the pore created are reported in Table 2.

In the cases where test voltages did not lead to the creation of the pore (for simulation times (t_{sim}) exceeding 60 ns), we concluded that the electroporation threshold $U_{EPthres}$ was higher. We defined therefore the latter as lying between the U_t values where the pores have not occurred and the U_t values where we observed the pore creation. The $U_{EPthres}$ intervals found for archaeal lipids are reported in Fig. 5 and compared to those DPPC, DPhPC-ester and -ether derived from a previous study [24].

4. Discussion

In the present study we investigated the properties and electroporation thresholds of bilayers formed by archaeal lipids (AI and AGI) and their mixtures with DPPC using MD simulations. Prior to the examination of the response to electrical stress of these bilayers, we have compared their structural characteristics to those determined by small angle X-ray scattering. The electron density profiles derived from MD simulations were found to agree very well with the ones determined from SAXS measurements providing therefore some confidence in the force fields and protocols adopted in the simulations.

The configurational sampling of the lipids partitioning in a mixed composition bilayer is a very slow process, and there is always a nagging question whether the results of finite time simulations depend on the initial membrane configuration. One possibility to overcome this
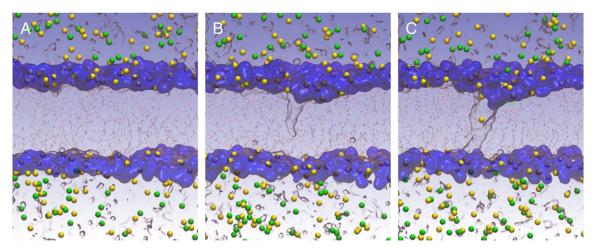
Fig. 4. Electroporation of archaeal lipid bilayers (snapshots at successive times after imposing a transmembrane voltage above the threshold): A) initial configuration, B) formation of water wire and C) formation of conducting 'hydrophobic' pore (white — lipid tails (between lipid headgroups), blue — lipid headgroups, yellow — potassium ion, green — chloride ion, water — gray surface).

would be to perform MD simulations using coarse grain models [50], but today, there are not yet robust force-fields to represent archaeal lipids. Here we have assumed that the AI at this concentration (10 mol% lipid content) does not aggregate but partition uniformly in the bilayer. We have then mainly relied on the comparison of the structural features to SAXS data to gain some confidence in the membrane model.

Before proceeding with the study of the archaeal lipids electroporation we have sought to determine and check some key properties of the bilayers. Among these, the dipole potential and capacitance as we have previously shown can be directly estimated from simulations and compared to experiments. The charge and molecular dipole distributions in the anisotropic lipid bilayers are at the origin of an intrinsic electrostatic profile (EP) across the membrane. In their pioneering work [51], from the measurements of the partition coefficients of fat-soluble tetraphenylboron anions and fat-soluble triphenylphosphonium cations between the membrane and aqueous phases, Liberman and Topaly hypothesized that the inner part of the bilayer membrane must be initially positively charged. The absolute value of this "dipole potential" has been very difficult to measure or predict [52–54], and estimates obtained from various methods and for various lipids range from 200 to 1000 mV. More recent and direct measurement based on Cryo-EM
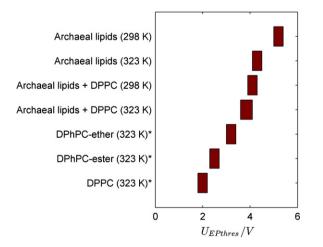
imaging [54] and atomic force microscopy (AFM) [55] techniques showed that the dipole potential can be "measured" in a noninvasive manner and estimate its value to few 100 mV. The large body of data from the simulations of fully hydrated lipid bilayers is found in qualitative agreement with experiments, showing that the EP profile monotonically increases across the membrane–water interface [41,42,54,56,57]. Given the diversity of the lipids studied and more significantly of the force fields used, values of dipole potentials ranging from 500 to 1200 mV have been reported [46,53,54,58–60]. The dipole potential measured here for archaeal lipids were found in this range (~200 mV). Though direct estimates from experiments for membranes of this composition are not available, it is worth to note that the results we obtained in a recent study for diphytanoyl-PC (DPhPC) [24], a lipid with tails similar to those of the archaeal lipids amount to 700 mV and 360 mV for the ester and ether forms which matches very well the data from [54] 510 mV and 260 mV, respectively. In particular the force fields used are good enough to reproduce the 50% decrease in the dipole potential from ester to ether lipids.

The MD protocols used here allow one also to estimate the capacitance of the bilayer at specific ionic strength and for a given salt composition. Here, the value found for the archaeal lipids, to the best of our knowledge not determined yet experimentally amounts to 0.7 μF cm^{-2}, which is in within the magnitude of the capacitances found in similar systems (DPhPC). Taken together, these initial analyses of the MD simulations strengthen our confidence in the force fields used as far as the electrostatic properties of the membranes modeled here are concerned.

Accordingly, these protocols were further used to study the stability of archaeal lipids bilayers and their mixtures with DPPC when subject to transmembrane voltages using a method mimicking the effect of low magnitude microsecond electric pulses [25,47]. The electroporation thresholds ($U_{EPthres}$) found here are probably overestimated as are all the electroporation thresholds determined so far from MD simulations [25,49]. Indeed, the $U_{EPthres}$ of planar lipid bilayers formed of phospholipids estimated using simulations are above 1.5 V [24,25,61] while the experimentally measured voltage breakdown of planar lipid bilayers ranges rather from 200 mV to 600 mV [62]. The reasons behind such large discrepancies are to date unclear.

At any rate, our calculations show that the archaeal lipid membranes have a much higher $U_{EPthres}$ than all other bilayers composed of simple phospholipids studied so far. The properties of lipids which contribute to the stability of membranes might be numerous and diverse, but include at least (a) the structure of the lipid tails, (b) the chemical nature of the head group and (c) the nature of the head to tail linkage

Fig. 5. Electroporation thresholds ($U_{EPthres}$) intervals determined from the MD simulations for the archaeal lipids and their mixtures with DPPC at 298 and 323 K. $U_{EPthres}$ of DPPC, DPhPC-ester and DPhPC-ether were adopted from [24]*.

(ester or ether). The studied archaeal lipids have special head groups carrying inositol and glucose functions. In comparison to simple phosphatidylcholine (PC) head groups these carbohydrates are larger moieties that move much more slowly. Furthermore and as importantly, the carbohydrates in the lipid head groups are packed and are involved in hydrogen bonds. As clearly evident from the data (Fig. 5) and comparing $U_{EPthres}$ between DPhPC and archaeal lipids, these special head group moieties contribute substantially to the increase of these bilayers electroporation thresholds.

More so the head-group/head-group and tail/tail moieties interactions in a membrane composed of lipid mixtures play a key, yet not evident role in their electrical stability. Uitert et al. [63] showed for instance that stability of lipid membranes composed of two types of lipids is not necessarily linearly dependent on the concentration of one species, highlighting the fact that the behavior of mixtures cannot easily be predicted. Other examples are found in the literature. For instance, the electrical stability of POPC membranes increases with the addition of cholesterol up to 50% [64], while the stability of DPhPC membranes increases with addition of cholesterol only up to 10%, then decreases at higher concentration: at cholesterol ratios of ~50%, the electrical stability of DPhPC is even lower than stability of pure DPhPC [63].

The archaeal lipids studied here have very complex structure in comparison to the DPPC or even DPhPC. It is very hard to predict, how the electrical stability of their mixtures with a second component (here DPPC) vary with the lipid composition. The DPPC lipid tails are not as long as those of archaeal lipids and they are formed of simple acyl chains. It is unclear how their zwittterionic and smaller head groups affect the bilayer electrical stability. Both characteristics namely influence the packing of the lipids in the bilayer.

Shinoda et al. have performed an extensive study of water permeability [65] in DPPC and DPhPC bilayers that may perhaps provide a rationale for the increased electroporation threshold, due to branched lipid tails. The authors show from analyses of local diffusion coefficients that water molecules have considerably reduced mobility in the DPhPC membrane interior as compared with the DPPC membrane interior. As a result of reduced water diffusion in the branch-chained membrane, the water permeability of the DPhPC bilayer was less than that of the DPPC bilayer by about 30%. As such permeability or diffusion toward the interior of the membrane is the very initial and key step in electroporation, we expect that this has a direct incidence on $U_{EPthres}$. One note along these lines that our previous study of bilayers composed of DPhPC-
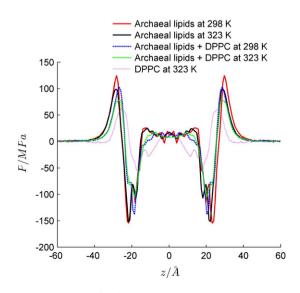
ester showed the increase of $U_{EPthres}$ compared to DPPC bilayers due to change in the lipid tails composition [24].

Seeking to identify how such characteristics can change in the electroporation thresholds, we have computed the lateral pressure profiles of the archaeal lipid membranes and their mixtures with DPPC and pure DPPC (Fig. 6). The profiles show higher peaks in hydrophilic head group region as well as in the hydrophobic core region. The same effect was observed at comparison of DPPC and DPhPC lipids [24]. One may speculate in line with our previous finding that a direct implication of such characteristics is also to lower the permeability of water and therefore to increase the electroporation threshold. Similarly, the temperature, another key factor in the lipid chains mobility is shown here to affect $U_{EPthres}$.

In contrast, the capacitances of the bilayers studied here do not seem to correlate to any extent with the electroporation thresholds, since these were found essentially unchanged with bilayers composition. Counter intuitively also to what was expected, the bilayers dipole potentials magnitudes are not directly correlated with the value of $U_{EPthres}$. These dipole potentials are proportional to the strength of the electric field at the bilayer headgroup/water interfaces. The one of archaeal lipid bilayers is much lower than that of pure PC lipids and increases with increasing concentration of DPPC lipids in the mixtures, while the thresholds of electroporation subsequently decrease.

5. Conclusion

In this study we showed that archaeal lipids with their special moieties i.e. methyl groups in tails, ether linkages instead of ester linkages and carbohydrates in the head groups have much higher stability than other simple lipids studied so far. We also showed that by mixing the archaeal lipids with phospholipids, one can lower their stability. Tuning in the electroporation threshold by lipid composition provides new routes for the design of liposomes composition that can be efficiently used as drug delivery carriers, and for which quantitatively monitored electroporation can serve for subsequent release of the drug when the carrier has reached proper location.

Abbreviations

T	temperature
t_{sim}	simulation time
A_m	area per lipid molecule
U_d	membrane dipole potential
C_{sp}	specific capacitance of bilayer
Q_{im}	charge imbalance
U_t	transmembrane voltage
t_{sim}	simulation time
t_{water}	time when first water wire is formed
t_{ion}	time when first ions goes through the pore

Fig. 6. The lateral pressure profile of archaeal lipid bilayers and their mixtures with DPPC in 0.45 mol l^{-1} KCl and at 298 and 323 K and the DPPC bilayers at 323 K.

References

[1] T. Benvegnu, M. Brard, D. Plusquellec, Archaeabacteria bipolar lipid analogues: structure, synthesis and lyotropic properties, Curr. Opin. Colloid Interface Sci. 8 (2004) 469–479.

[2] N.P. Ulrih, D. Gmajner, P. Raspor, Structural and physicochemical properties of polar lipids from thermophilic archaea, Appl. Microbiol. Biotechnol. 84 (2009) 249–260.

[3] N.P. Ulrih, U. Adamlje, M. Nemec, M. Sentjurc, Temperature- and pH-induced structural changes in the membrane of the hyperthermophilic archaeon *Aeropyrum pernix* K1, J. Membr. Biol. 219 (2007) 1–8.

[4] Y. Sako, N. Nomura, A. Uchida, Y. Ishida, H. Morii, Y. Koga, et al., *Aeropyrum pernix* gen. nov., sp. nov., a novel aerobic hyperthermophilic archaeon growing at temperatures up to 100 °C, Int. J. Syst. Bacteriol. 46 (1996) 1070–1077.

[5] H. Morii, H. Yagi, H. Akutsu, N. Nomura, Y. Sako, Y. Koga, A novel phosphoglycolipid archaetidyl(glucosyl)inositol with two sesterterpanyl chains from the aerobic hyperthermophilic archaeon *Aeropyrum pernix* K1, Biochim. Biophys. Acta, Mol. Cell. Biol. Lipids 1436 (1999) 426–436.

[6] M.J. Hanford, T.L. Peeples, Archaeal tetraether lipids: unique structures and applications, Appl. Biochem. Biotechnol. 97 (2002) 45–62.

[7] T.A. Elbayoumi, V.P. Torchilin, Current trends in liposome research, Methods Mol. Biol. 605 (2010) 1–27.

[8] T.B. Napotnik, M. Rebersek, T. Kotnik, E. Lebrasseur, G. Cabodevila, D. Miklavcic, Electropermeabilization of endocytotic vesicles in B16 F1 mouse melanoma cells, Med. Biol. Eng. Comput. 48 (2010) 407–413.

[9] L. Retelj, G. Pucihar, D. Miklavcic, Electroporation of intracellular liposomes using nanosecond electric pulses—a theoretical study, IEEE Trans. Biomed. Eng. 60 (2013) 2624–2635.

[10] E. Neumann, K. Rosenheck, Permeability changes induced by electric impulses in vesicular membranes, J. Membr. Biol. 10 (1972) 279–290.

[11] S. Haberl, D. Miklavcic, G. Sersa, W. Frey, B. Rubinsky, Cell membrane electroporation-Part 2: the applications, IEEE Electr. Insul. Mag. 29 (2013) 29–37.

[12] M. Tarek, Membrane electroporation: a molecular dynamics simulation, Biophys. J. 88 (2005) 4045–4053.

[13] Z.A. Levine, P.T. Vernier, Life cycle of an electropore: field-dependent and field-independent steps in pore creation and annihilation, J. Membr. Biol. 236 (2010) 27–36.

[14] D.P. Tieleman, The molecular basis of electroporation, BMC Biochem. 5 (2004) 10.

[15] H. Leontiadou, A.E. Mark, S.-J. Marrink, Ion transport across transmembrane pores, Biophys. J. 92 (2007) 4209–4215.

[16] A. Cordomí, O. Edholm, J.J. Perez, Effect of ions on a dipalmitoyl phosphatidylcholine bilayer. A molecular dynamics simulation study, J. Phys. Chem. B 112 (2008) 1397–1408.

[17] M. Breton, L. Delemotte, A. Silve, L.M. Mir, M. Tarek, Transport of siRNA through lipid membranes driven by nanosecond electric pulses: an experimental and computational study, J. Am. Chem. Soc. 134 (2012) 13938–13941.

[18] E. Tekle, H. Oubrahim, S.M. Dzekunov, J.F. Kolb, K.H. Schoenbach, P.B. Chock, Selective field effects on intracellular vacuoles and vesicle membranes with nanosecond electric pulses, Biophys. J. 89 (2005) 274–284.

[19] T. Portet, C. Favard, J. Teissié, D.S. Dean, M.-P. Rols, Insights into the mechanisms of electromediated gene delivery and application to the loading of giant vesicles with negatively charged macromolecules, Soft Matter 7 (2011) 3872.

[20] P. Kramar, D. Miklavcic, A.M. Lebar, Determination of the lipid bilayer breakdown voltage by means of linear rising signal, Bioelectrochemistry 70 (2007) 23–27.

[21] T. Portet, F. Camps i Febrer, J.-M. Escoffre, C. Favard, M.-P. Rols, D.S. Dean, Visualization of membrane loss during the shrinkage of giant vesicles under electropulsation, Biophys. J. 96 (2009) 4109–4121.

[22] M.J. Ziegler, P.T. Vernier, Interface water dynamics and porating electric fields for phospholipid bilayers, J. Phys. Chem. B 112 (2008) 13588–13596.

[23] P.T. Vernier, Z.a. Levine, M.a. Gundersen, Water bridges in electropermeabilized phospholipid bilayers, Proc. IEEE 101 (2013) 494–504.

[24] A. Polak, D. Bonhenry, F. Dehez, P. Kramar, D. Miklavčič, M. Tarek, On the electroporation thresholds of lipid bilayers: molecular dynamics simulation investigations, J. Membr. Biol. 246 (2013) 843–850.

[25] L. Delemotte, M. Tarek, Molecular dynamics simulations of lipid membrane electroporation, J. Membr. Biol. 245 (2012) 531–543.

[26] R. a Böckmann, B.L. de Groot, S. Kakorin, E. Neumann, H. Grubmüller, Kinetics, statistics, and energetics of lipid membrane electroporation studied by molecular dynamics simulations, Biophys. J. 95 (2008) 1837–1850.

[27] D. Needham, R.M. Hochmuth, Electro-mechanical permeabilization of lipid vesicles. Role of membrane tension and compressibility, Biophys. J. 55 (1989) 1001–1009.

[28] M.L. Fernández, G. Marshall, F. Sagués, R. Reigada, Structural and kinetic molecular dynamics study of electroporation in cholesterol-containing bilayers, J. Phys. Chem. B 114 (2010) 6855–6865.

[29] I. Milek, B. Cigic, M. Skrt, G. Kaletunç, N.P. Ulrih, Optimization of growth for the hyperthermophilic archaeon Aeropyrum pernix on a small-batch scale, Can. J. Microbiol. 51 (2005) 805–809.

[30] D. Gmajner, A. Ota, M. Sentjurc, N.P. Ulrih, Stability of diether C(25,25) liposomes from the hyperthermophilic archaeon *Aeropyrum pernix* K1, Chem. Phys. Lipids 164 (2011) 236–245.

[31] E.G. Bligh, W.J. Dyer, A rapid method of total lipid extractin and purification, Can. J. Biochem. Physiol. 37 (1959) 911–917.

[32] O. Kratky, H. Stabinger, X-ray small angle camera with block-collimation system an instrument of colloid research, Colloid Polym. Sci. 262 (1984) 345–360.

[33] D. Orthaber, A. Bergmann, O. Glatter, SAXS experiments on absolute scale with Kratky systems using water as a secondary standard, J. Appl. Crystallogr. 33 (2000) 218–225.

[34] O. Glatter, A new method for the evaluation of small-angle scattering data, J. Appl. Crystallogr. 10 (1977) 415–421.

[35] O. Glatter, Evaluation of small-angle scattering data from lamellar and cylindrical particles by the indirect transformation method, J. Appl. Crystallogr. 13 (1980) 577–584.

[36] D.J. Iampietro, L.L. Brasher, E.W. Kaler, A. Stradner, O. Glatter, Direct analysis of SANS and SAXS measurements of catanionic surfactant mixtures by Fourier transformation, J. Phys. Chem. B 102 (1998) 3105–3113.

[37] T. Sato, H. Sakai, K. Sou, M. Medebach, O. Glatter, E. Tsuchida, Static structures and dynamics of hemoglobin vesicle (HBV) developed as a transfusion alternative, J. Phys. Chem. B 113 (2009) 8418–8428.

[38] O. Glatter, Convolution square root of band-limited symmetrical functions and its application to small-angle scattering data, J. Appl. Crystallogr. 14 (1981) 101–108.

[39] O. Glatter, B. Hainisch, Improvements in real-space deconvolution of small-angle scattering data, J. Appl. Crystallogr. 17 (1984) 435–441.

[40] R. Mittelbach, O. Glatter, Direct structure analysis of small-angle scattering data from polydisperse colloidal particles, J. Appl. Crystallogr. 31 (1998) 600–608.

[41] J.B. Klauda, R.M. Venable, J.A. Freites, J.W. O'Connor, D.J. Tobias, C. Mondragon-Ramirez, et al., Update of the CHARMM all-atom additive force field for lipids: validation on six lipid types, J. Phys. Chem. B 114 (2010) 7830–7843.

[42] K. Shinoda, W. Shinoda, T. Baba, M. Mikami, Comparative molecular dynamics study of ether- and ester-linked phospholipid bilayers, J. Chem. Phys. 121 (2004) 9648–9654.

[43] L. Kalé, R. Skeel, M. Bhandarkar, R. Brunner, A. Gursoy, N. Krawetz, et al., NAMD2: greater scalability for parallel molecular dynamics, J. Comput. Phys. 151 (1999) 283–312.

[44] U. Essmann, L. Perera, M.L. Berkowitz, T. Darden, H. Lee, L.G. Pedersen, A smooth particle mesh Ewald method, J. Chem. Phys. 103 (1995) 8577.

[45] T. Darden, D. York, L. Pedersen, Particle mesh Ewald: an N·log(N) method for Ewald sums in large systems, J. Chem. Phys. 98 (1993) 10089.

[46] J.N. Sachs, P.S. Crozier, T.B. Woolf, Atomistic simulations of biologically realistic transmembrane potential gradients, J. Chem. Phys. 121 (2004) 10847–10851.

[47] L. Delemotte, F. Dehez, W. Treptow, M. Tarek, Modeling membranes under a transmembrane potential, J. Phys. Chem. B 112 (2008) 5547–5550.

[48] E. Lindahl, O. Edholm, Spatial and energetic–entropic decomposition of surface tension in lipid bilayers from molecular dynamics simulations, J. Chem. Phys. 113 (2000) 3882.

[49] P. Kramar, L. Delemotte, A. Maček Lebar, M. Kotulska, M. Tarek, D. Miklavčič, Molecular-level characterization of lipid membrane electroporation using linearly rising current, J. Membr. Biol. 245 (2012) 651–659.

[50] H.I. Ingólfsson, C.a. Lopez, J.J. Uusitalo, D.H. de Jong, S.M. Gopal, X. Periole, et al., The power of coarse graining in biomolecular simulations, Wiley Interdiscip. Rev. Comput. Mol. Sci. 00 (2013).

[51] E. Liberman, V. Topaly, Permeability of bimolecular phospholipid membranes for fat-soluble ions, Biophysics (1968) 477–487.

[52] R.J. Clarke, The dipole potential of phospholipid membranes and methods for its detection, Adv. Colloid Interface Sci. 89–90 (2001) 263–281.

[53] A.P. Demchenko, S.O. Yesylevskyy, Nanoscopic description of biomembrane electrostatics: results of molecular dynamics simulations and fluorescence probing, Chem. Phys. Lipids 160 (2009) 63–84.

[54] L. Wang, P.S. Bose, F.J. Sigworth, Using cryo-EM to measure the dipole potential of a lipid membrane, Proc. Natl. Acad. Sci. U. S. A. 103 (2006) 18528–18533.

[55] Y. Yang, K.M. Mayer, N.S. Wickremasinghe, J.H. Hafner, Probing the lipid membrane dipole potential by atomic force microscopy, Biophys. J. 95 (2008) 5193–5199.

[56] K. Gawrisch, D. Ruston, J. Zimmerberg, V. a Parsegian, R.P. Rand, N. Fuller, Membrane dipole potentials, hydration forces, and the ordering of water at membrane surfaces, Biophys. J. 61 (1992) 1213–1223.

[57] U. Peterson, D. a Mannock, R.N.A.H. Lewis, P. Pohl, R.N. McElhaney, E.E. Pohl, Origin of membrane dipole potential: contribution of the phospholipid fatty acid chains, Chem. Phys. Lipids 117 (2002) 19–27.

[58] M.L. Berkowitz, D.L. Bostick, S. Pandit, Aqueous solutions next to phospholipid membrane surfaces: insights from simulations, Chem. Rev. 106 (2006) 1527–1539.

[59] R.J. Mashl, H.L. Scott, S. Subramaniam, E. Jakobsson, Molecular simulation of dioleoylphosphatidylcholine lipid bilayers at differing levels of hydration, Biophys. J. 81 (2001) 3005–3015.

[60] A.M. Smondyrev, M.L. Berkowitz, Structure of dipalmitoylphosphatidylcholine/cholesterol bilayer at low and high cholesterol concentrations: molecular dynamics simulation, Biophys. J. 77 (1999) 2075–2089.

[61] P.T. Vernier, M.J. Ziegler, Y. Sun, M. a Gundersen, D.P. Tieleman, Nanopore-facilitated, voltage-driven phosphatidylserine translocation in lipid bilayers—in cells and in silico, Phys. Biol. 3 (2006) 233–247.

[62] M. Kotulska, P. Kramar, D. Miklavc, Voltage- and current-clamp methods for determination of planar lipid bilayer properties, in: A. Iglič (Ed.), Adv. Planar Lipid Bilayers Liposomes, vol. 11, Elsevier, Amsterdam, 2010, pp. 29–69.

[63] I. van Uitert, S. Le Gac, A. van den Berg, The influence of different membrane components on the electrical stability of bilayer lipid membranes, Biochim. Biophys. Acta 1798 (2010) 21–31.

[64] M. Naumowicz, Z.A. Figaszewski, Pore formation in lipid bilayer membranes made of phosphatidylcholine and cholesterol followed by means of constant current, Cell Biochem. Biophys. 66 (2013) 109–119.

[65] W. Shinoda, M. Mikami, T. Baba, M. Hato, Molecular dynamics study on the effects of chain branching on the physical properties of lipid bilayers: 2. Permeability, J. Phys. Chem. B 108 (2004) 9346–9356.

Andraž Polak was born in 1986. He received his B.Sc. degree in Electrical Engineering from the University of Ljubljana, Slovenia, in 2010. He is currently a Ph.D. student in the Department of Biomedical Engineering at the Faculty of Electrical Engineering of the University of Ljubljana. His current research interests include electroporation of planar lipid bilayers on experimental and modeling level.

Nataša Poklar Ulrih was born in 1965. She received a Ph.D. in Physical Chemistry from the University of Ljubljana, Slovenia, in 1994. She is a full professor of Biochemistry, head of the Chair of Biochemistry and Food Chemistry, and vice-dean of the Department of Food Science and Technology at the Biotechnical Faculty, University of Ljubljana. During the last few years she is interested in the molecular mechanism of adaptation of archaea to extreme environmental conditions.

Mounir Tarek was born in 1964. He received a Ph.D. (1994) in Physics from the University of Paris. He is currently a senior research scientist (Directeur de Recherches) of the CNRS at the University of Lorraine, France. He joined the CNRS after 3 years as a postdoctoral scientist at the University of Pennsylvania, and a 4-year tenure at the National Institute of Standards and Technology, Gaithersburg, Maryland. During the last few years, he has worked on large-scale, state-of-the-art molecular simulations of lipid membranes and transmembrane proteins, probing their structure and dynamics.

Andrej Jamnik was born in 1961. He received his Ph.D. in Chemistry from the University of Ljubljana, Slovenia, in 1992. Currently he is a full professor of Physical Chemistry in the Faculty of Chemistry and Chemical Technology at the University of Ljubljana. His research focuses on the investigations of thermodynamic and structural properties of simple fluids, solutions and colloidal dispersions using theoretical methods based on principles of statistical mechanics (integral equation theories and computer simulations) and complementing experimental techniques based on scattering of light and X-rays.

Matija Tomšič was born in 1976. He received a Ph.D. on the Faculty of Chemistry and Chemical Technology (FKKT UL), University of Ljubljana, Slovenia, in 2004. He is currently a lecturer on the Chair of Physical Chemistry on the FKKT UL. After his studies he specialized in the field of light scattering methods and their application in structural research of various colloidal systems. His current research interests include structural aspects of bacterial polysaccharide systems, calculating small-wide-angle X-ray scattering (SWAXS) data of modeled liquids and their validation by experimental SWAXS results.

Peter Kramar was born in 1977. He received a Ph.D. in Electrical Engineering from the University of Ljubljana, Slovenia, in 2010. He is currently a teaching assistant in the Faculty of Electrical Engineering at the University of Ljubljana. His current research interests include electroporation of planar lipid bilayers.

Janez Valant was born in 1979. He received his Ph.D. in biochemistry and molecular biology at University of Ljubljana in 2010. He is currently employed as a postdoctoral scientist at University of Ljubljana, Biotechnical faculty. His current research interest includes toxicological aspects of nanoparticles, especially interactions of nanoparticles with lipid membranes.

Damijan Miklavčič was born in 1963. He received a Ph.D. in Electrical Engineering from the University of Ljubljana, Slovenia in 1993. He is currently a full professor, head of the Laboratory of Biocybernetics, and head of the Department of Biomedical Engineering at the Faculty of Electrical Engineering of the University of Ljubljana. During the last few years his research has been focused on electroporation-based gene transfer and drug delivery, development of electronic hardware, and numerical modeling of biological processes.